Abnormal Expression of the Steroid Hormone Synthesis Pathway Associates with Cattle Ovarian Cysts

Xiaoling Xu
Institute of Animal Husbandry and Veterinary Medicine, Beijing Academy of Agriculture and Forestry Science

Jiahua Bai
Institute of Animal Husbandry and Veterinary Medicine, Beijing Academy of Agriculture and Forestry Science

Yusheng Qin
Institute of Animal Husbandry and Veterinary Medicine, Beijing Academy of Agriculture and Forestry Science

Tao Feng
Institute of Animal Husbandry and Veterinary Medicine, Beijing Academy of Agriculture and Forestry Science

Linli Xiao
Institute of Animal Husbandry and Veterinary Medicine, Beijing Academy of Agriculture and Forestry Science

Yuqing Song
Institute of Animal Husbandry and Veterinary Medicine, Beijing Academy of Agriculture and Forestry Science

Ting Yang
Institute of Animal Husbandry and Veterinary Medicine, Beijing Academy of Agriculture and Forestry Science

Yan Liu (liuyanxms@163.com)
Animal Husbandry and Veterinary Medicine, Beijing Academy of Agriculture and Forestry Science

---

Research

Keywords: hormonal profiling, steroid hormone synthesis, ovarian cysts, RNA-seq, ELISA

Posted Date: February 17th, 2021

DOI: https://doi.org/10.21203/rs.3.rs-201894/v1

Abstract

Background

When a mature follicle fails to ovulate, ovarian cysts can develop and persist in the ovary, interfering with normal ovarian functions. However, the etiology of ovarian cysts remains poorly understood.

Results

By enzyme-linked immunosorbent assay (ELISA) of the bovine follicle fluid from cystic follicles , we found that cystic follicles were characterized by lower oestradiol (E_2), Insulin-like growth factor 1(IGF1), and insulin levels but elevated progesterone (P_4) compared with preovulatory follicles (p <0.05). Further gene expression profiling of follicle walls by RNA sequencing (RNA-seq) showed that there are 356 differentially expressed genes between preovulatory follicles and corpus luteum cyst groups, and 582 differentially expressed genes between preovulatory follicles and follicular cyst groups. Kyoto Encyclopedia of Genes and Genomes (KEGG) analysis linked steroid hormone synthesis pathway to the formation of ovarian cysts, and steroidogenic acute regulatory protein (*STAR*), cytochrome P450, family 11, subfamily A, polypeptide 1 (*CYP*11*A*1), hydroxy-delta-5-steroid dehydrogenase, 3-beta- and steroid delta-isomerase 1 (*HSD*3*B*1), cytochrome P450, family 17, subfamily A, polypeptide 1 (*CYP*17*A*1), and cytochrome P450, family 1, subfamily B, polypeptide 1 (*CYP*1*B*1) genes in the steroid hormone synthesis pathway play important roles in this process.

Conclusions

Abnormal hormone profiles and expression of steroid hormone synthesis pathway genes related to the formation of ovarian cysts. The findings lay a theoretical foundation for the prevention and treatment of ovarian cysts.

Background

Ovarian cysts are the most common reproductive dysfunction in high-producing dairy cows, causing significant economic losses to the dairy industry by extending the calving stage, increasing days in the postpartum period, and lengthening the replacement rate due to infertility (1, 2). Ovarian cysts are defined as follicle-like structures present on one or both ovaries, with a diameter of at least 2.0 cm for a minimum of 10 days (3). Ovarian cysts can be classified functionally as follicular or luteal, and follicular cysts have a relatively thin wall (£3 mm) and lack any evidence of luteal tissue, while luteal cysts have thicker walls (>3 mm) (4).

Studies over many years have shown that the formation of ovarian cysts is mainly the result of hormonal imbalance within the hypothalamic-pituitary-gonadal axis caused by endogenous and/or exogenous factors (3, 5, 6). The most widely accepted hypothesis explaining the formation of a cyst is that luteinizing hormone (LH) release from the hypothalamus-pituitary is altered, and the pre-ovulatory LH

surge is either absent, insufficient in magnitude, or occurs at the wrong time during dominant follicle maturation, leading to cyst formation (7, 8, 9). Meanwhile, progesterone (P_4) is involved in the formation of ovarian cysts, and there is a strong association between intermediate concentrations of P_4 in peripheral blood and the occurrence of ovarian follicular cysts (3). Most cysts are accompanied by a decrease of P_4, which promotes the development of the cyst (10). Molecular analysis of bovine cystic ovarian disease pathogenesis has revealed that ovaries in animals with ovarian cysts exhibit disrupted steroid receptor patterns related to follicle-stimulating hormone receptor (*FSHR*), progesterone receptor (*PGR*), LH/choriogonadotropin receptor (*LHCGR*), and estrogen receptor (*ESR*) (1, 11, 12).

Negative energy balance (NEB) is another factor that can also lead to the formation of ovarian cysts (6). Imbalance between energy intake through feed and energy expenditure through milk yield during the early postpartum period causes NEB, which is usually accompanied by hormonal and metabolic adaptations that affect ovarian function (13,14). During NEB, circulating concentrations of insulin-like growth factor 1 (IGF1), insulin (13), and leptin (15, 16) are reduced. Zulu et al. (17) reported that low systemic IGF-1 concentrations in early postpartum may contribute to anovulation and subsequent development of cystic follicles, while Vanholder et al. (18) reported that reduced circulating insulin concentrations in early postpartum may play a role in ovarian dysfunction (i.e. cyst formation). Spicer (2001) hypothesized that above a certain threshold level, leptin acts as a trigger to initiate hypothalamo-pituitary gonadotropin secretion. In a moderate to high leptin environment, as occurs in obesity, leptin limits ovarian steroidogenesis (19). These findings indicate that the molecular mechanism of the formation of ovarian cysts in dairy cows is complicated.

With the development of advanced molecular genetics technologies, especially next-generation sequencing and bioinformatics, transcriptome sequencing (RNA-seq) provides a convenient platform for measuring large-scale gene expression patterns in organisms (20). The fine detail provided by sequencing-based transcriptome approaches indicates that RNA-seq is likely to become the platform of choice for interrogating steady-state RNA levels, and RNA-seq also enables the detection of differentially expressed genes (DEGs) with low expression levels (21, 22). Some studies have analyzed the transcriptome profiles of liver samples from lactating dairy cows divergent in NEB (23), and the anterior pituitary of heifers before and after ovulation (24).

However, RNA-seq has not yet been widely employed for determination of large-scale gene expression patterns to explain the molecular mechanism of ovarian cyst formation. Therefore, the present study aimed to investigate hormonal and gene expression patterns in follicular and luteal cysts compared with normal preovulatory follicles (controls) via enzyme-linked immunosorbent assay (ELISA) and deep sequencing of the transcriptome to identify novel genes and their associated biological pathways that are important in ovarian cysts in cattle.

Material And Methods

Animals and clinical diagnosis of ovarian cysts

All cows were from local dairy farms in Beijing. First, the ovarian conditions of nonpregnant lactating cows were monitored daily by ultrasonography using a Honda HS1600V real-time B-mode scanner equipped with a 7.5 MHz linear-array trans-rectal transducer (Honda, Toyohashi, Japan). Based on the ultrasound image, in the absence of active luteal tissue, a follicle structure diameter >20 mm for more than 15 days with a thin wall (≤3 mm) and uniformly anechogenic follicular fluid was defined as a follicular cyst, while a thicker wall (>3 mm) with a visible echogenic rim, spots, and web-like structures signified a corpus luteum cyst (25). Holstein cows with normal preovulatory follicles on day 18 after synchronization of estrus and without reproductive disorders were assigned to the control group.

Tissue sampling, follicular fluid collection, and processing

Following B-ultrasound diagnosis, cyst and preovulatory follicles were obtained from cows during slaughter at a nearby abattoir, and rinsed in ice-cold saline (0.9% NaCl). The follicular fluid (one sample collected from 1 cow) of the upper follicles was extracted, centrifuged at 2000 rpm for 10 min, the supernatant was collected in sterilized Eppendorf tubes, the follicular wall was exfoliated and immediately preserved in liquid nitrogen, and samples were stored at -80°C until further analysis.

Measurement of hormone concentrations in follicular fluid

ELISA was conducted to measure the concentrations of oestradiol, P_4, insulin and IGF-1 levels in follicular fluids. All ELISA kits were purchased from the Jiancheng Bioengineering Institute (Nanjing, China), and assays were performed according to the manufacturer's instructions. Briefly, 50 μL of standards or samples were added to the appropriate well of the microtiter plate pre-coated with antibody, gently mixed, and incubated for 60 min at 37°C. After washing, biotinylated anti-IgG and streptavidin-horseradish peroxidase (HRP) were added along with chromogen solutions A and B. Finally, the optical density (OD) at 450 nm was recorded using a Multiskan MK3 automatic microplate spectrophotometer (Thermo Fisher Scientific, Waltham, MA, USA). Hormone concentrations were calculated according to standard curves, and each experiment was repeated independently at least three times.

RNA extraction, library preparation, and sequencing

Total RNA was extracted from follicular walls using TRIzol reagent (Invitrogen, Carlsbad, CA, USA) according to the manufacturer's instructions, and RNA was purified using an miRNeasy kit (Qiagen, Hilden, Germany). Sequencing and bioinformatics analysis were conducted by Beijing Genomics Institute (BGI; Beijing, China). The quality of RNA was assessed using an Agilent 2100 Bioanalyzer system (Agilent Technologies, Palo Alto, CA, USA) and samples with a RNA integrity number (RIN) >8 were used for RNA library construction. Briefly, polyA+ mRNA was purified using oligo-dT-attached magnetic beads. Selected mRNAs were fragmented and reverse-transcribed to double-stranded cDNA (dscDNA) using N6 random primers. Ends of dscDNAs were repaired with phosphate at the 5' end and A at the 3' end to ligate with

adaptors with T at the 3’ end of dscDNAs, which were subjected to amplification (26). RNA-seq libraries were sequenced on a BGISEQ-500 instrument (BGI; www.genomics.org.cn). Detailed procedures have been published previously (27). Raw reads have been deposited in the National Center for Biotechnology Information (NCBI) Sequence Read Archive database (https://www.ncbi.nlm.nih.gov/sra) under accession number PRJNA602176

Bioinformatics analysis

Raw RNA-seq data were filtered into clean reads, followed by mapping against the *Bos taurus* reference genome (mm10) using HISAT (28). Gene expression levels were quantified using the RSEM software package (29). DEGs between control and cyst groups were identified using fold change ≥2 and false discovery rate (FDR) ≤0.001 as criteria. Gene Ontology (GO) annotation was used to map all DEGs to GO terms in the database (http://www.geneontology.org/), and GO terms with Q-values (corrected *p*-value) ≤0.05 defined DEGs as significantly enriched. The Kyoto Encyclopedia of Genes and Genomes (KEGG) database was used to perform pathway enrichment analysis of DEGs, and pathway terms with Q-values ≤0.05 were defined as significantly enriched (30).

Statistical analysis

All data are presented as mean percentages ± standard error of the mean (SEM) from a minimum of three independent replicate experiments. Different groups were analyzed by SPSS version 12.0 (SPSS, Chicago, IL, USA) and significant differences between means were determined using the least significant difference (LSD) test for comparison of multiple means. Statistical significance was defined at $p < 0.05$.

Results

Hormonal and metabolic profiling of follicular fluid

Different ovarian conditions were monitored daily by ultrasonography, and typical ovarian cysts and preovulatory follicles were obtained from Holstein cows during slaughter at a nearby abattoir. Ultrasound images and *in vitro* ovarian images are shown in Figure 1.

Concentrations of hormones in follicular fluids of follicular cysts (n = 30), corpus luteum cysts (n = 21) and normal preovulatory follicles (n = 19) were assayed by ELISA methods, and the hormonal profiles are presented in Table 1. Firstly, as expected, preovulatory follicles were characterized by high oestradiol (503.89 ± 48.29 pg/mL) and low progesterone (83.68 ± 12.35 ng/mL) concentrations. Follicular cyst follicles had lower oestradiol (320.71 ± 49.78 pg/mL) and almost equal P_4 (84.65 ± 12.69 ng/mL) levels compared with preovulatory follicles, while corpus luteum cyst follicles had lower oestradiol (189.01 ± 27.54 pg/mL) and higher P_4 (588.87 ± 98.28 ng/mL) levels than preovulatory follicles. Secondly, the insulin concentration was 56.97 ± 0.90 mIU/mL for preovulatory follicles, compared with 20.14 ± 5.06

mIU/mL and 22.35 ± 2.89 mIU/mL for follicular and corpus lutein cysts, respectively. Differences between preovulatory follicles and cysts were significant (p <0.05). The IGF-1 concentration was 175.94 ± 11.48 ng/mL in preovulatory follicles, compared with 107.79 ± 8.316 ng/mL and 132.40 ± 11.82 ng/mL in follicular and corpus lutein cysts, respectively. The average concentration of follicular fluid IGF-1 in follicles with ovarian cysts was significantly lower than in preovulatory follicles (p <0.05).

Table 1
Hormonal patterns in follicle fluid from preovulatory and cyst follicles

Groups	Estradiol (pg/mL)	Progesterone (P_4) (ng/mL)	Insulin (mIU/mL)	insulin-like growth factor 1 (IGF1) (ng/mL)
Preovulatory follicles (n = 19)	503.89 ± 48.29^a	83.68 ± 12.35^b	56.97 ± 0.90^b	175.94 ± 11.48^a
Follicular cysts (n = 30)	320.71 ± 49.78^b	84.65 ± 12.69^b	20.14 ± 5.06^a	107.79 ± 8.32^c
Corpus luteum cysts (n = 21)	189.01 ± 27.54^c	588.87 ± 98.28^a	22.35 ± 2.89^a	132.40 ± 11.82^b
Note: Within a column, means followed by different superscript letters are significantly different.				

Sequencing data summary

In this study, nine RNA samples from three different follicle wall tissues, namely follicular cysts (F1-F3), corpus luteum cysts (L1-L3), and normal preovulatory follicle controls (C1-C3), were subjected to deep sequencing using an Illumina HiSeq1500 platform. For each sample, ~20 million raw reads were generated, yielding at least 15 million mapped reads (Table 2). After being filtered, clean reads were mapped to the bovine reference genome using HISAT 10 and Bowtie2 (http://bowtie-bio.sourceforge.net/Bowtie2 /index.shtml). The average mapping ratio with reference genes was 92.85%, and separate mapping rates for each sample are listed in Table 3.

Table 2
Overview transcriptome data and mapped reads

Sample	Total raw reads (M)	Total clean reads (M)	Total clean bases (Gb)	Clean reads Q20 (%)	Clean reads Q30 (%)	Clean reads ratio (%)
C-1	67.47	67.47	6.75	98.07	90.93	100
C-2	62.46	62.46	6.25	97.33	89.16	100
C-3	71.88	71.88	7.19	97.26	89.24	100
F-1	23.4	23.4	1.17	98.68	92.52	100
F-2	69.9	69.9	6.99	97.32	89.38	100
F-3	69.52	69.52	6.95	97.98	90.63	100
L-1	69.7	69.7	6.97	97.31	89.36	100
L-2	23.91	23.91	1.2	98.54	92.01	100
L-3	23.77	23.77	1.19	98.5	91.72	100

Table 3
Alignment statistics for reads aligned to the reference genome

Sample	Total clean reads	Total mapping ratio	Uniquely mapping ratio
C-1	67473682	94.66%	92.09%
C-2	62461656	93.68%	90.95%
C-3	71881880	94.45%	91.52%
F-1	46799794	93.93%	82.07%
F-2	69904126	94.15%	91.02%
F-3	69516870	94.78%	92.21%
L-1	69696216	94.41%	92.00%
L-2	47829380	94.64%	84.07%
L-3	47531822	93.56%	83.90%

Identification of expressed genes and DEGs

A total of 31097 expressed genes were detected in all three samples for preovulatory follicles and ovarian cyst groups. Gene expression levels were quantified by RSEM, and the number of identified expressed genes in each sample is shown in Figure 2. The Venn diagram shows gene expression levels among the

different groups. The number of co-expressed genes was 38,466, and the number of specifically expressed genes was 1254, 2520, and 1118 for preovulatory follicles, follicular cysts, and luteum cysts, respectively (Figure 3).

Based on the fragments per kilobase of transcript per million mapped reads (FPKM) values of all expressed genes, Pearson's correlation values were calculated for pairwise comparisons among samples, and were >0.90 among the three biological replicates for control and cyst groups. A total of 356 genes displayed differential expression between control and corpus luteum cyst groups, among which 197 and 159 DEGs were up- and down-regulated, respectively (Figure 4). A total of 582 genes displayed differential expression between control and follicular cyst groups, among which 471 and 111 DEGs were up- and down-regulated, respectively (Figure 4). The correlation coefficient between different samples was also investigated, and luteal cysts exhibited the lowest correlations with other groups (Figure 5).

Clustering analysis of DEGs

In order to identify the functions of DEGs in cyst vs. control and corpus luteum cyst vs. control groups, GO analysis was performed based on three functional categories; biological process (BP), cellular component (CC), and molecular function (MF), and the results are shown in Figure 6A and 6B. Regarding BP classes, DEGs (149 genes for cyst vs. control and 97 genes for corpus luteum cyst vs. control groups, respectively) related to cellular process were the most enriched and DEGs (100 genes for cyst vs. control and 74 genes for luteum cyst vs. control groups, respectively) related to biological regulation constituted the second largest group. Regarding CC classes, DEGs associated with cell (166 genes and 99 genes), cell part (166 genes and 99 genes) and organelle (131 genes and 92 genes) were the top enriched. Finally, most MF classes were linked to binding activity (124 and 84 genes) and catalytic activity (66 genes and 47 genes).

Pathway enrichment analysis of DEGs

Genes often interact with each other to mediate specific biological functions. Pathway enrichment analysis of DEGs was therefore performed on DEGs using the KEGG database, and DEGs identified in the follicular cyst vs. control and corpus luteum cyst vs. control group comparisons were mapped to KEGG metabolic and regulatory pathways with a correct *p*-value cutoff of $p < 0.05$. The top 20 KEGG enrichment results are shown in Figure 7A and 7B. From the pathway analysis, steroid hormone synthesis was linked to the formation of ovarian cysts.

Key DEGs associated with the formation of ovarian cysts

Pathway analysis showed that the steroid hormone synthesis pathway is associate with the formation of both follicular and luteum cysts. Thus, the expression of key genes involved in this signaling pathway

was further analyzed. The results showed that steroidogenic acute regulatory protein (*STAR*), cytochrome P450, family 11, subfamily A, polypeptide 1 (*CYP*11*A*1), and hydroxy-delta-5-steroid dehydrogenase, 3-beta- and steroid delta-isomerase 1 (*HSD3B*1) were up-regulated significantly (p <0.05) while cytochrome P450, family 17, subfamily A, polypeptide 1 (*CYP*17*A*1) and cytochrome P450, family 1, subfamily B, polypeptide 1 (*CYP*1*B*1) were down-regulated (p <0.05).

Table 4
Expression of key DEGs associated with the formation of ovarian cysts

Gene	Gene ID	Preovulatory follicles (FPKM)	Follicular cysts (FPKM)	Corpus luteum cysts (FPKM)
Steroid hormone synthesis pathway				
Bos taurus steroidogenic acute regulatory protein (*STAR*)	281,507	37.69 (1.37)	557.92 (21.14)	114.27 (4.78)
Bos taurus cytochrome P450, family 11, subfamily A, polypeptide 1 (*CYP*11*A*1)	338,048	23 (1.43)	1151 (64.87)	120 (6.51)
Bos taurus hydroxy-delta-5-steroid dehydrogenase, 3-beta- and steroid delta-isomerase 1 (*HSD3B*1)	281,824	40 (2.47)	340 (21.84)	62 (4.39)
Bos taurus cytochrome P450, family 17, subfamily A, polypeptide 1 (*CYP*17*A*1)	281,739	41 (2.4)	7 (0.43)	33 (2.21)
Bos taurus cytochrome P450, family 1, subfamily B, polypeptide 1 (*CYP*1*B*1)	511,470	114 (5.85)	25 (1.16)	41 (1.84)
Note: FPKM means Fragments Per Kilobase per Million.				

Discussion

In the current study, we performed hormonal and metabolic profiling of bovine ovarian cysts, and identified DEGs by comparing normal (control) tissues with follicular and luteum cyst samples. It is known that dominant follicle selection is followed by ovulation (31). Follicle-stimulating hormone (FSH) induces antral follicle growth, associated with elevated estradiol production, and high estradiol levels enhance hypothalamic gonadotropin-releasing hormone (GnRH) pulses, triggering a surge in LH surge (32). However, decreased estradiol levels and a failed pre-ovulatory LH surge at the appropriate time during maturation of the dominant follicle leads to the formation of ovarian cysts (1, 33). Herein, hormonal profiling showed that, compared with dominant follicles, the ratios of estradiol to P_4 intrafollicular steroid levels in ovarian cysts were decreased significantly (p <0.05). Braw-Tal et al. (34) reported that preovulatory follicles are characterized by high estradiol and low P_4 concentrations, and the

estradiol-to-P_4 (E/P) ratio in these follicles was 42, but this ratio drops sharply to 0.91 in corpus luteum cysts. Follicular cysts contain greater P_4 (p <0.05) but lower estradiol (p <0.05) levels than noncystic follicles (35). An imbalance between estradiol and P_4 in intrafollicular fluids leads to the formation of ovarian cysts.

Hypothalamic-pituitary function and follicular growth and development may be affected by NEB through metabolic and/or hormonal adaptations. Insulin and IGF-1 have been postulated as key mediators between nutritional status and ovarian function in cattle (36, 37, 38). *In vitro* and *in vivo* studies on cows indicate that insulin and IGF-1 stimulate both estradiol synthesis in granulosa cells and androgen synthesis in theca cells (39, 40). Herein, the average IGF-1 concentration in follicular fluids of follicular cysts was significantly lower than in fluids from preovulatory follicles. Therefore, reduced insulin and IGF-1 levels may affect the follicular responsiveness to LH stimulation, which could lead to anovulation and cyst formation.

Abnormal secretion of steroid hormones and metabolic factors can explain the formation of ovarian cysts, but the specific molecular mechanism remains unknown. Some researchers reported that follicular cysts appear to be associated with changes in the transcription of *IRs*, *IGFRs* (18), *PAPP-A* (41), and *HSD3B*1 and LH receptor genes (42), as well as reduced localization of estrogen receptor β protein and increased localization of estrogen receptor α protein (43). Kisspeptin may also be involved in the pathogenesis of bovine follicular cysts (44). Cows with ovarian cysts display abnormal steroidogenic markers (*LHCGR*, *StAR*, *CYP*11*A*1, 3β-*HSD*, *CYP*19*A*), immunological markers (*IL*-1β, *IL*-6, *IL*-8, *TLR*-4, *TNF*), and metabolic markers (*IGF*-1, *IRS*1) (9). However, high-throughput studies on the formation of ovarian cysts are lacking. A previous microarray analysis investigated gene expression in granulosa cells from dominant and cystic follicles collected from dairy cows by ultrasound-guided aspiration, revealing 163 DEGs (p <0.01), of which 19 were up-regulated and 144 were down-regulated (35). High-throughput RNA-seq is even more powerful for identifying DEGs. In the present study, large-scale gene expression patterns were determined to analyze the molecular mechanism of ovarian cysts. The results revealed that steroid hormone synthesis was linked to the formation of ovarian cysts. In particular, the expression of *STAR*, *CYP*11*A*1, *HSD3B*1 *CYP*17*A*1, and *CYP*1*B*1 genes in related to the steroid hormone synthesis pathway plays an important role in the formation of ovarian cysts.

Conclusion

In conclusion, abnormal hormone profile and gene expression of the steroid hormone synthesis pathway associates with cattle ovarian cysts. Coupled with previous studies, our current work comparing cystic and normal preovulatory follicles greatly expands our knowledge in this area, but further investigation is needed to determine cause-and-effect relationships. Therefore, future research should focus on changes occurring during follicle growth that may interfere with normal follicle development and steroidogenesis, and lead to the formation of cysts.

Abbreviations

ELISA: enzyme-linked immunosorbent assay

E_2: oestradiol

IGF1: Insulin-like growth factor 1

P_4: progesterone

RNA-seq: RNA sequencing

KEGG: Kyoto Encyclopedia of Genes and Genomes

STAR: steroidogenic acute regulatory protein

CYP11A1: cytochrome P450, family 11, subfamily A, polypeptide 1

HSD3B1: hydroxy-delta-5-steroid dehydrogenase, 3-beta- and steroid delta-isomerase 1

CYP17A1: cytochrome P450, family 17, subfamily A, polypeptide 1

CYP1B1: cytochrome P450, family 1, subfamily B, polypeptide 1

LH: luteinizing hormone

FSHR: follicle-stimulating hormone receptor

PGR: progesterone receptor

LHCGR: LH/choriogonadotropin receptor

ESR: estrogen receptor

NEB: negative energy balance

DEGs: differentially expressed genes

HRP: streptavidin-horseradish peroxidase

OD: optical density

RIN: RNA integrity number

FSH: Follicle-stimulating hormone

GnRH: gonadotropin-releasing hormone

Declarations

Availability of data and materials

The data supporting the conclusions of this article is included within the article and its additional file.

Acknowledgements

Many thanks to Jianhui Tian (China Agricultural university, China) for the guidance of B-ultrasonic diagnosis.

Funding

This work was supported by the Beijing Innovation Team of Technology System in Dairy Industry (grant number BAIC06-2021), the Scientific & Technological Innovation Ability Construction Project of the Beijing Academy of Agriculture and Forestry Science (grant number KJCX20200209), and funding from the National Natural Science Foundation of China (grant number 31301975).

Author information

Xiaoling Xu and Jiahua Bai contributed equally to this work.

Affiliations

Laboratory of Animal Production, Institute of Animal Husbandry and Veterinary Medicine, Beijing Academy of Agriculture and Forestry Sciences, Beijing, BJ, China

Author contributions

Xiaoling Xu performed experiments, analyzed data, and wrote the manuscript. Jiahua Bai performed experiments and analyzed data. Yusheng Qin performed the ELISA experiment. Tao Feng helped with tables and figures. Linli Xiao and Yuqing Song lead the B-ultrasonic diagnosis of ovarian samples at the farm. Ting Yang collected ovaries from slaughterhouses. Yan Liu conceived of and designed experiments and analyzed the sequence data. All authors contributed to writing the manuscript and approved the final manuscript.

Corresponding author

Correspondence to Yan Liu

Ethics declarations

Ethics approval and consent to participate

Protocols and procedures related to animal work in this study were approved by the Institutional Animal Care and Use Committee (IACUC) of the Institute of Animal Husbandry and Veterinary Medicine, Beijing Academy of Agriculture and Forestry Sciences, China (approval number IACUC-2010).

Consent for publication

Not applicable.

Competing interests

The authors declare that they have no competing interests.

References

1. **Peter AT**. An update on cystic ovarian degeneration in cattle. *Reprod Domest Anim* 39(1):1-7, 2004.
2. **Ortega HH, Marelli BE, Rey F, Amweg AN, Díaz PU, Stangaferro ML, Salvetti NR**. Molecular aspects of bovine cystic ovarian disease pathogenesis. *Reproduction* 149 (6):R251-64, 2015. doi: 10.1530/REP-14-0618.
3. **Silvia WJ, Hatler TB, Nugent AM, Laranja da Fonseca LF**. Ovarian follicular cysts in dairy cows: an abnormality in folliculogenesis. *Domest Anim Endocrinol* 23(1-2):167-77, 2002.
4. **Kesler DJ, Garverick HA**. Ovarian cysts in dairy cattle: a review. *J Anim Sci* 55(5):1147-59, 1982.
5. **Cook DL, Parfet JR, Smith CA, Moss GE, Youngquist RS, Garverick HA**. Secretory patterns of LH and FSH during development and hypothalamic and hypophysial characteristics following development of steroid-induced ovarian follicular cysts in dairy cattle. *J Reprod Fert* 91:19-28, 1991.
6. **Vanholder T, Opsomer G, de Kruif A**. Aetiology and pathogenesis of cystic ovarian follicles in dairy cattle: a review. *Reprod Nutr Dev* 46(2):105-19, 2006.
7. **Hamilton SA, Garverick HA, Keisler DH, Xu ZZ, Loos K, Youngquist RS, Salfen BE.** Characterization of ovarian follicular cysts and associated endocrine profiles in dairy cows. *Biol Reprod* 53: 890-98, 1995.
8. **Yoshioka K, Iwamura S, Kamomae H**. Ultrasonic observations on the turnover of ovarian follicular cysts and associated changes of plasma LH, FSH, progesterone and oestradiol-17β in cows. *Res Vet*

Sci 61: 240-244, 1996.

9. **Lima FS, Acosta DAV, Egan TR, Skenandore C, Sulzberger S, French DD, Cardoso FC**. Steroidogenic, Metabolic, and Immunological Markers in Dairy Cows Diagnosed With Cystic Ovarian Follicles at Early and Mid-Late Lactation. *Front Vet Sci* 6:324, 2019. doi: 10.3389/fvets.2019.00324.
10. **Hatler TB, Hayes SH, Laranja da Fonseca LF, Silvia WJ**. Relationship between endogenous progesterone and follicular dynamics in lactating dairy cows with ovarian follicular cysts. *Biol Reprod* 69(1):218-23, 2003.
11. **Salvetti NR, Stangaferro ML, Palomar MM, Alfaro NS, Rey F, Gimeno EJ, Ortega HH**. Cell proliferation and survival mechanisms underlying the abnormal persistence of follicular cysts in bovines with cystic ovarian disease induced by ACTH. *Anim Reprod Sci* 122(1-2):98-110, 2010. doi: 10.1016/j.anireprosci.2010.08.003.
12. **Marelli BE, Diaz PU, Salvetti NR, Rey F, Ortega HH**. mRNA expression pattern of gonadotropin receptors in bovine follicular cysts. *Reprod Biol* 14(4):276-81, 2014. doi: 10.1016/j.repbio.2014.08.002.
13. **Beam SW, Butler WR**. Effects of energy balance on follicular development and first ovulation in postpartum dairy cows. *J Reprod Fertil Suppl* 54:411-24, 1999.
14. **Opsomer G, Gröhn YT, Hertl J, Coryn M, Deluyker H, de Kruif A**. Risk factors for post partum ovarian dysfunction in high producing dairy cows in Belgium: a field study. *Theriogenology* 53(4):841-57, 2000.
15. **Block SS, Butler WR, Ehrhardt RA, Bell AW, Van Amburgh ME, Boisclair YR**. Decreased concentration of plasma leptin in periparturient dairy cows is caused by negative energy balance. *J Endocrinol* 171:339-48, 2001.
16. **Liefers SC, Veerkamp RF, te Pas MFW, Delavaud C, Chilliard Y, van der Lende T**. Leptin concentrations in relation to energy balance, milk yield, intake, live weight, and estrus in dairy cows. *J Dairy Sci* 86: 799-807, 2003.
17. **Zulu VC, Sawamukai Y, Nakada K, Kida K, Moriyoshi M**. Relationship among Insulin-Like Growth Factor-I, Blood metabolites and Post Partum Ovarian Function in Dairy cows. *J Vet Med Sci* 64: 879-85, 2002.
18. **Vanholder T, Leroy JL, Dewulf J, Duchateau L, Coryn M, de Kruif A, Opsomer G**. Hormonal and metabolic profiles of high-yielding dairy cows prior to ovarian cyst formation or first ovulation post partum. *Reprod Domest Anim* 40(5):460-7, 2005.
19. **Spicer LJ**. Leptin: a possible metabolic signal affecting reproduction. *Domest Anim Endocrin* 21: 251-70, 2001.
20. **Zhang D, Shang T, Huang Y, Wang S, Liu H, Wang J, Wang Y, Ji H, Zhang R**. Gene expression profile changes in the jejunum of weaned piglets after oral administration of Lactobacillus or an antibiotic. *Sci Rep* 7(1):15816, 2017. doi: 10.1038/s41598-017-16158-y.
21. **Robinson MD, Oshlack A**. A scaling normalization method for differential expression analysis of RNA-seq data. *Genome Biol* 11(3): R25, 2010. doi: 10.1186/gb-2010-11-3-r25.

22. **Tarazona S, García-Alcalde F, Dopazo J, Ferrer A, Conesa A**. Differential expression in RNA-seq: a matter of depth. *Genome Res* 21(12):2213-23, 2011. doi: 10.1101/gr.124321.111.
23. **McCabe M, Waters S, Morris D, Kenny D, Lynn D, Creevey C**. RNA-seq analysis of differential gene expression in liver from lactating dairy cows divergent in negative energy balance. *BMC Genomics*. 13:193, 2012. doi: 10.1186/1471-2164-13-193.
24. **Pandey K, Mizukami Y, Watanabe K, Sakaguti S, Kadokawa H**. Deep sequencing of the transcriptome in the anterior pituitary of heifers before and after ovulation. *J Vet Med Sci* 79 (6):1003-1012, 2017. doi: 10.1292/jvms.16-0531.
25. **Jeffcoate IA, Ayliffe TR**. An ultrasonographic study of bovine cystic ovarian disease and its treatment. *Vet Rec* 136(16):406-10, 1995.
26. **Hopkinson BM, Klitgaard MC, Petersen OW, Villadsen R, Rønnov-Jessen L, Kim J**. Establishment of a normal-derived estrogen receptor-positive cell line comparable to the prevailing human breast cancer subtype. *Oncotarget* 8(6):10580-593, 2017. doi: 10.18632/oncotarget.14554.
27. **Manchon L Chebli K Papon L Paul C Garcel A, Campos N, Scherrer D, Ehrlich H, Hahne M , Tazi J**. RNA sequencing analysis of activated macrophages treated with the anti-HIV ABX464 in intestinal inflammation. *Scientific data* 4:170150, 2017. doi: 10.1038/sdata.2017.150.
28. **Kim D, Langmead B, Salzberg SL**. HISAT: a fast spliced aligner with low memory requirements. *Nat Methods* 12 (4): 357-60, 2015. doi: 10.1038/nmeth.3317.
29. **Li B and Dewey CN**. RSEM: accurate transcript quantification from RNA-Seq data with or without a reference genome. *BMC bioinformatics* 12 (1): 323, 2011. doi: 10.1186/1471-2105-12-323.
30. **Kanehisa M, Araki M, Goto S, Hattori M, Hirakawa M, Itoh M, Katayama T, Kawashima S, Okuda S, Tokimatsu T, Yamanishi Y**. KEGG for linking genomes to life and the environment. *Nucleic Acids Res* 36 (Database issue):D480-4, 2008.
31. **Jaiswal RS, Singh J, Adams GP**. Developmental pattern of small antral follicles in the bovine ovary. *Biol Reprod* 71(4):1244-51, 2004.
32. **Richards JS, Pangas SA**. The ovary: basic biology and clinical implications, Review series. *J Clin Invest* 120:963-72, 2010. doi: 10.1172/JCI41350.
33. **Vanholder T, Opsomer G, Govaere JLJ, Coryn M, de Kruif A**. Cystic ovarian disease in dairy cattle: aetiology, pathogenesis, and risk factors. *Tijdschr. Diergeneesk* 127:146-155, 2002.
34. **Braw-Tal R Pen S Roth Z**. Ovarian cysts in high-yielding dairy cows. *Theriogenology* 72: 690-98, 2009. doi: 10.1016/j.theriogenology.2009.04.027.
35. **Grado-Ahuir JA, Aad PY, Spicer LJ**. New insights into the pathogenesis of cystic follicles in cattle: microarray analysis of gene expression in granulosa cells. *J Anim Sci* 89(6):1769-86, 2011. doi: 10.2527/jas.2010-3463.
36. **Diskin MG, Mackey DR, Roche JF, Sreenan JM**. Effect of nutrition and metabolic status on circulating hormones and ovarian follicle development in cattle. *Anim Reprod Sci* 78:345-70, 2003.

37. **Webb R, Garnsworthy PC, Gong J-G, Armstrong DG**. Control of follicular growth: local interactions and nutritional influences. *J Anim Sci* 82(Suppl): E63-74, 2004.
38. **Kawashima C, Fukihara S, Maeda M, Kaneko E, Montoya CA, Matsui M, Shimizu T, Matsunaga N, Kida K, Miyake Y, Schams D, Miyamoto A**. Relationship between metabolic hormones and ovulation of dominant follicle during the first follicular wave post-partum in high-producing dairy cows. *Reproduction* 133:155-63, 2007.
39. **Spicer LJ, Chamberlain CS, Maciel SM**. Influence of gonadotropins on insulin- and insulin-like growth factor-I (IGF-I)-induced steroid production by bovine granulosa cells. *Domest Anim Endocrin* 22: 237-254, 2002.
40. **Simpson RB, Chase CC, Spicer LJ, Vernon RK, Hammond AC, Rae DO**. Effect of exogenous insulin on plasma and follicular insulin-like growth factor I, insulin-like growth factor binding protein activity, follicular oestradiol and progesterone, and follicular growth in superovulated Angus and Brahman cows. *J Reprod Fertil* 102: 483-92, 1994.
41. **Rodríguez FM, Colombero M, Amweg AN, Huber E, Gareis NC, Salvetti NR, Ortega HH, Rey F**. Involvement of PAPP-A and IGFR1 in Cystic Ovarian Disease in Cattle. *Reprod Domest Anim* 50(4):659-68, 2015. doi: 10.1111/rda.12547.
42. **Calder MD, Manikkam M, Salfen BE, Youngquist RS, Lubahn DB, Lamberson WR, Garverick HA**. Dominant bovine ovarian follicular cysts express increased levels of messenger RNAs for luteinizing hormone receptor and 3β-hydroxysteroid dehydrogenase Δ 4, Δ 5 isomerase compared to normal dominant follicles. *Biol Reprod* 65:471-76, 2001.
43. **Salvetti NR, Acosta JC, Gimeno EJ, Müller LA, Mazzini RA, Taboada AF, Ortega HH**. Estrogen receptors α and β and progesterone receptors in normal bovine ovarian follicles and cystic ovarian disease. Vet Pathol 44:373-78, 2007.
44. **Rizzo A, Piccinno M, Ceci E, Pantaleo M, Mutinati M, Roncetti M, Sciorsci RL**. Kisspeptin and bovine follicular cysts. *Vet Ital* 54(1):29-31, 2018. doi: 10.12834/VetIt.1014.5413.3.

Figures

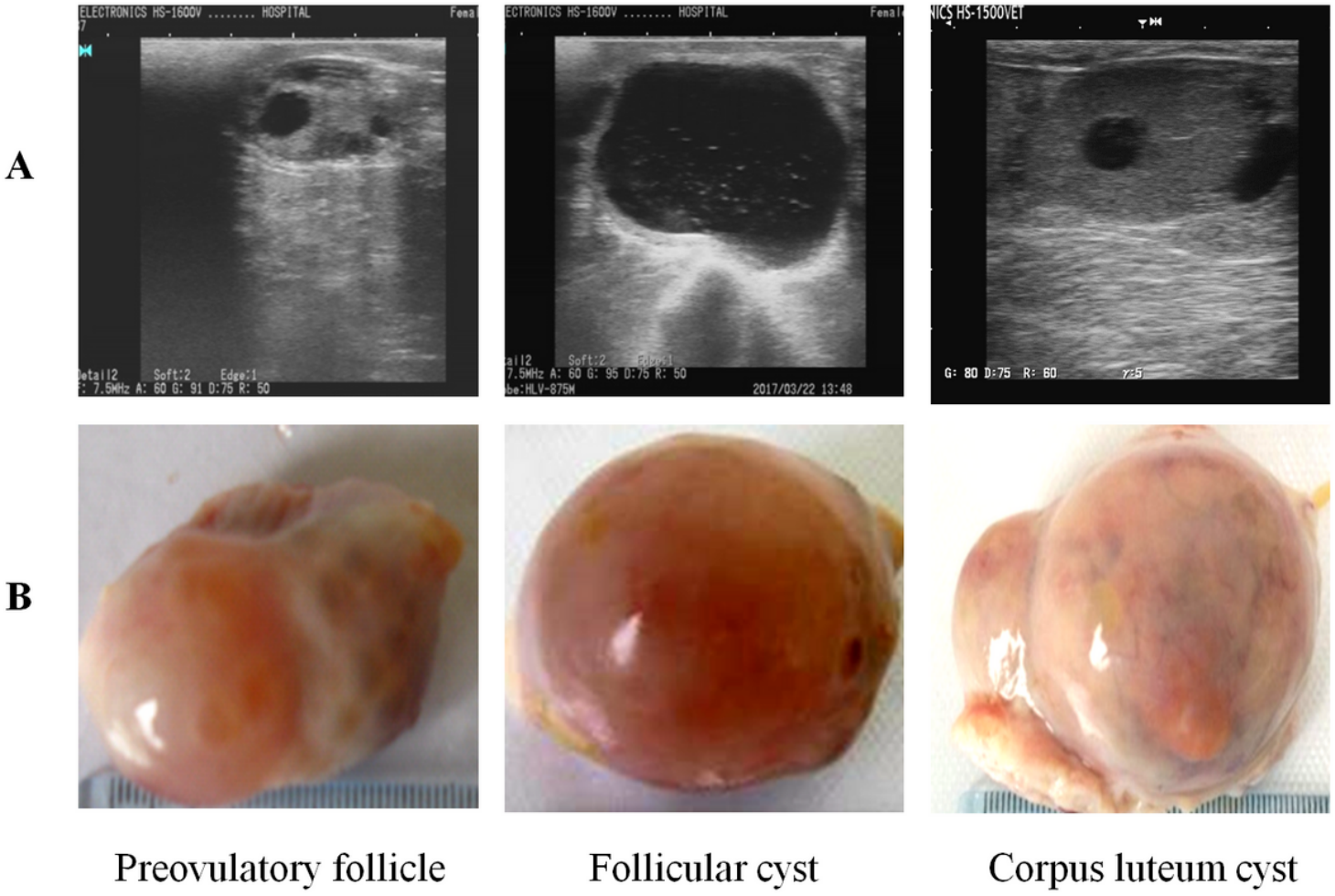

Figure 1

Typical ovarian cyst and preovulatory follicle ultrasound images (A) and physical photos (B).

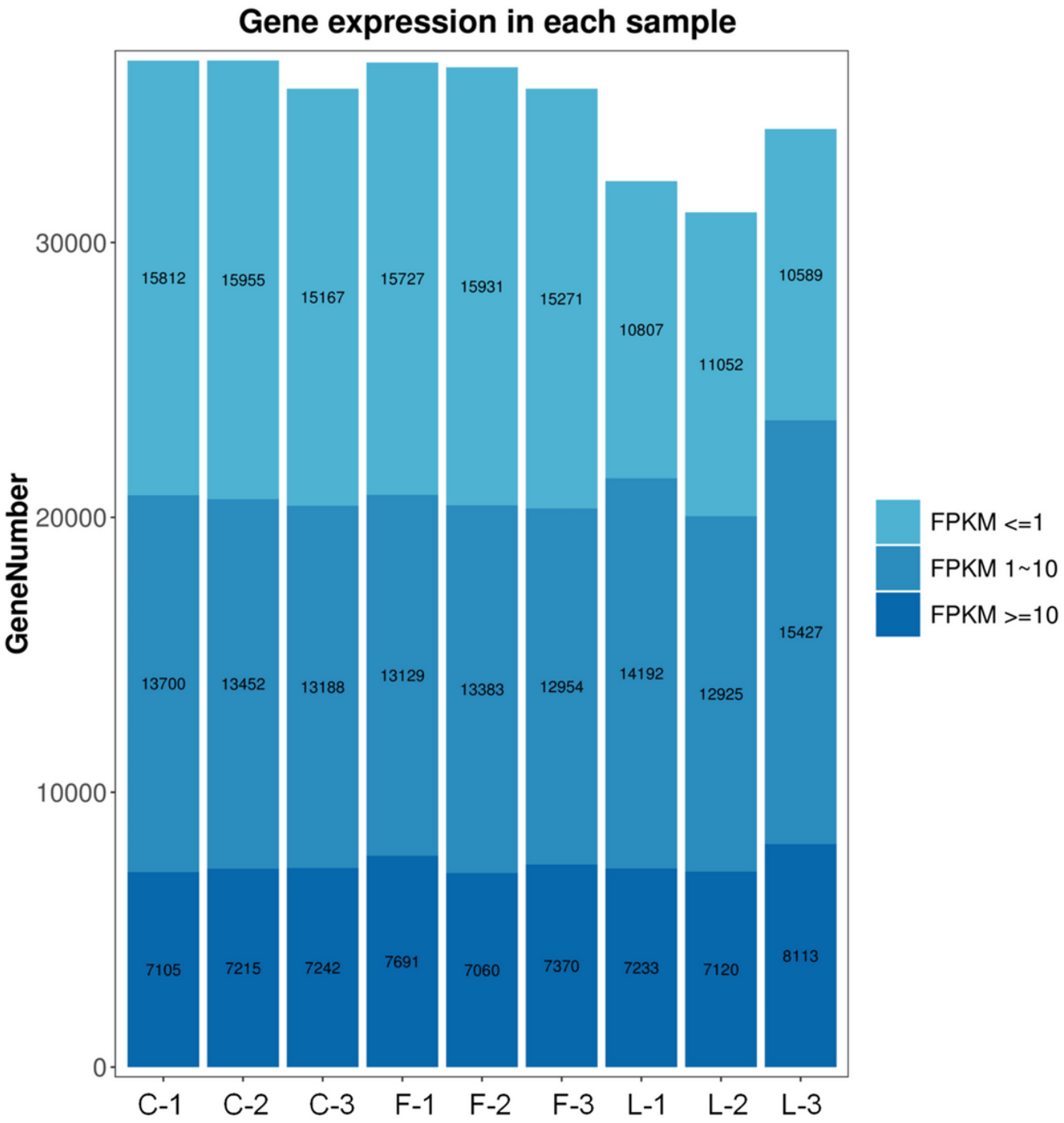

Figure 2

Gene expression map. The x-axis indicates the sample name and the y-axis indicates the number of identified expressed genes. The color depth indicates different expression level; FPKM ≤1 indicates genes with very low expression levels; FPKM between 1 and 10 indicates genes with low expression levels; FPKM ≥10 indicates genes with medium-to-high expression levels.

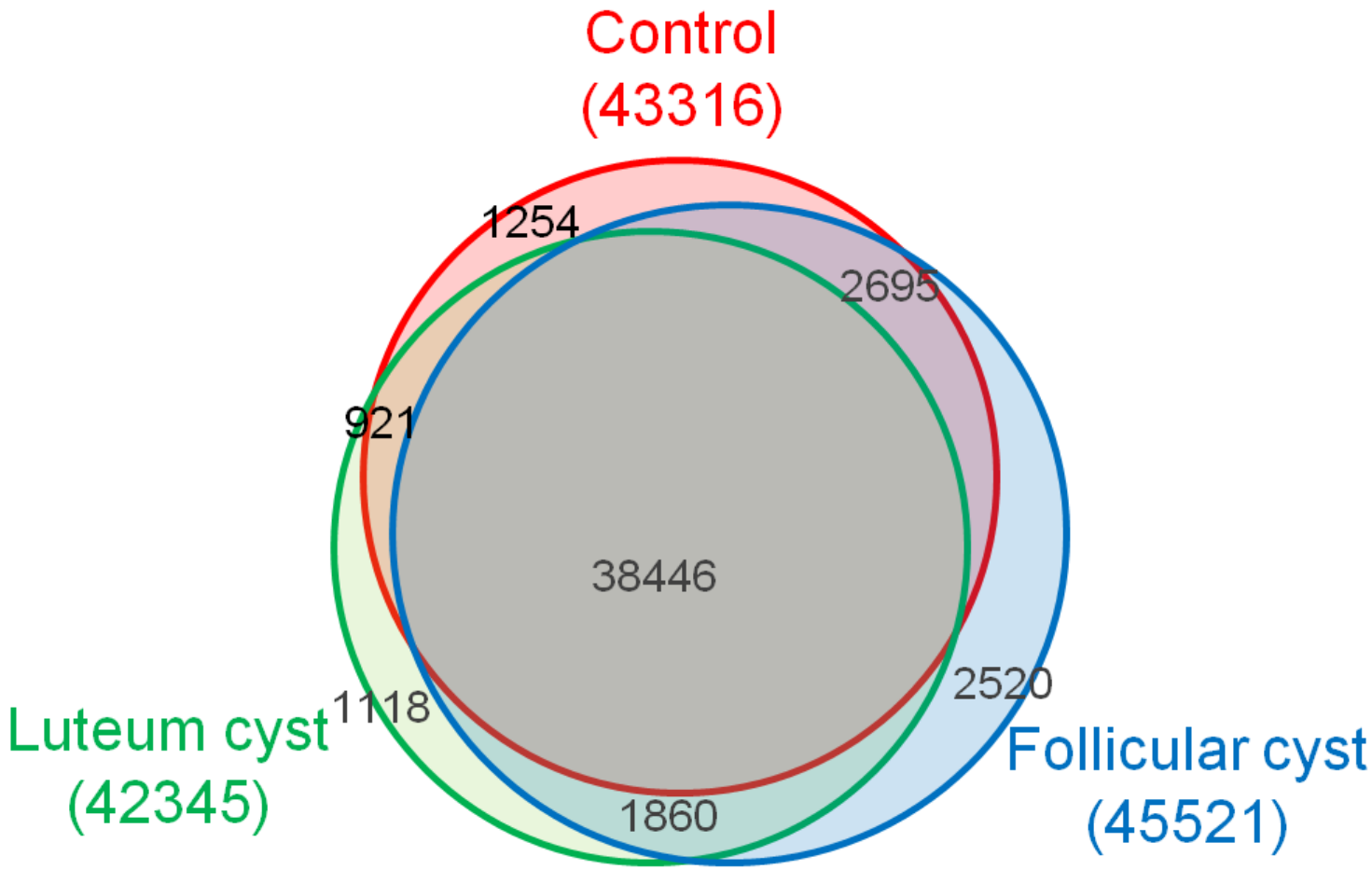

Figure 3

Venn diagram showing the number of co-expressed genes.

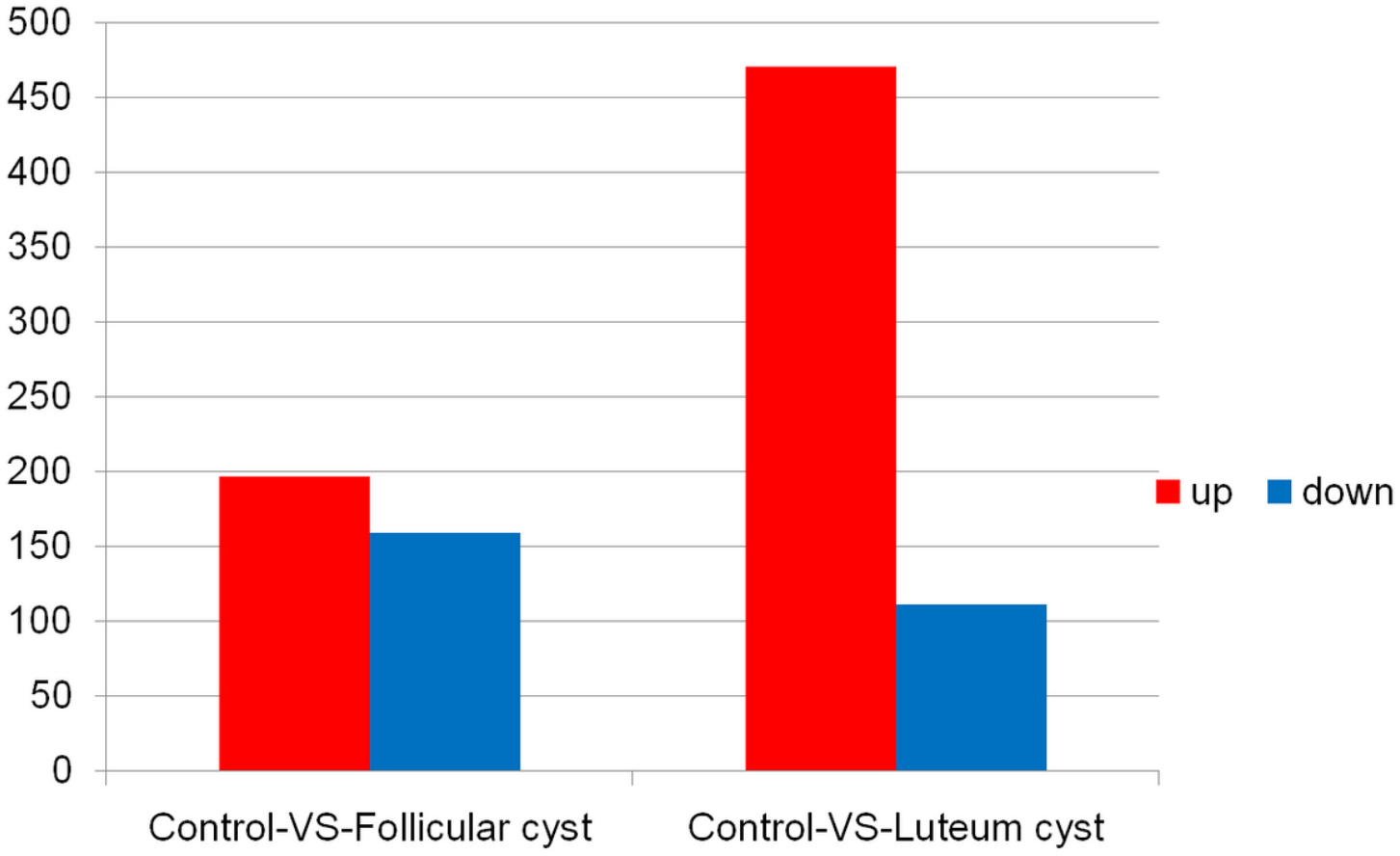

Figure 4

DEGs identified in control vs. follicular cyst and control vs. luteum cyst group comparisons. The x-axis represents pairwise comparisons and the y-axis shows the number of DEGs screened. Red bars denote up-regulated genes and blue bars are down-regulated genes.

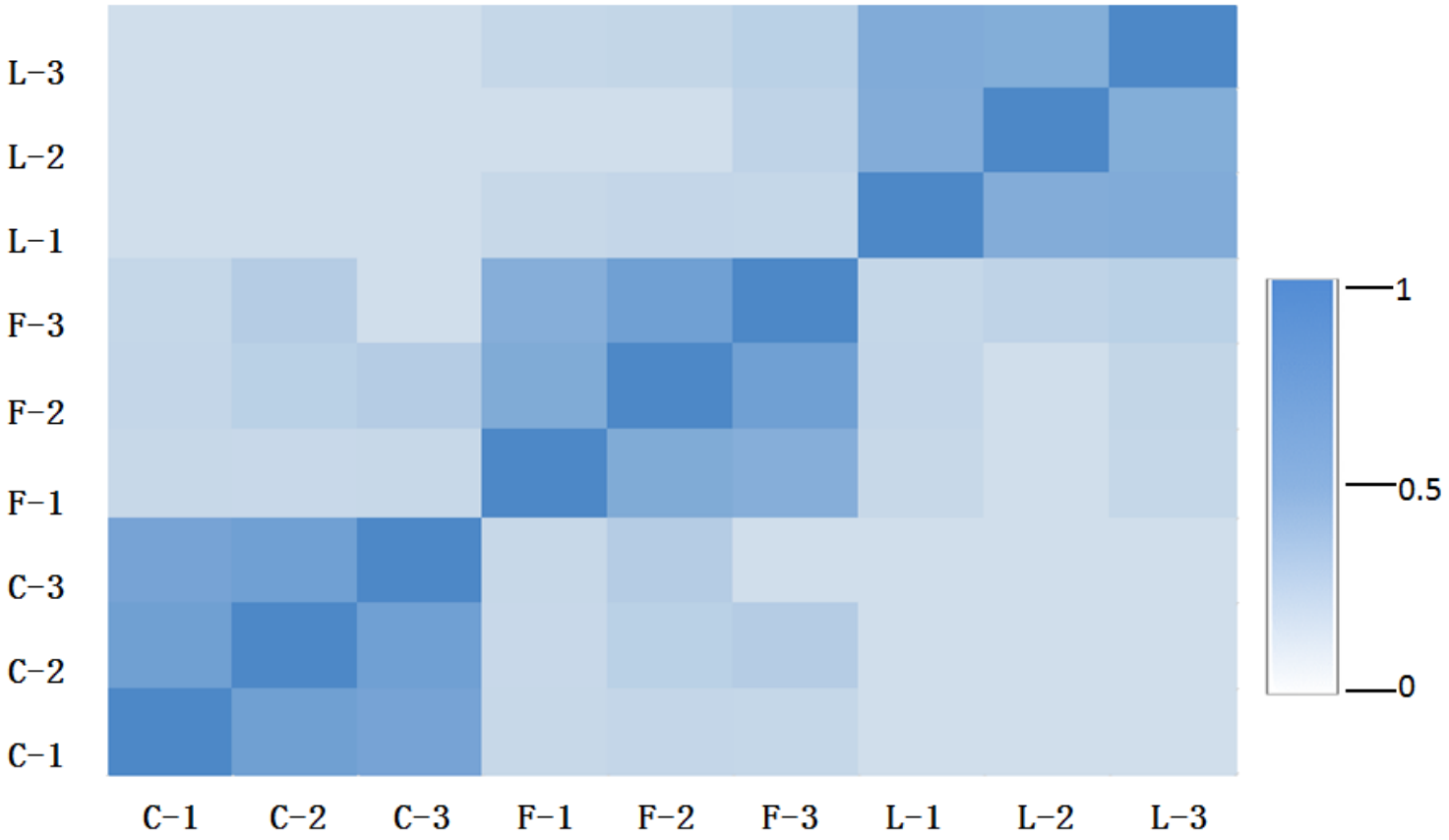

Figure 5

Heatmap of correlation coefficient values between samples. When the correlation value is close to 1, it indicates that the two samples are highly similar. The minimum and maximum values are indicated in white and blue, respectively, with a color gradient indicating intermediate values.

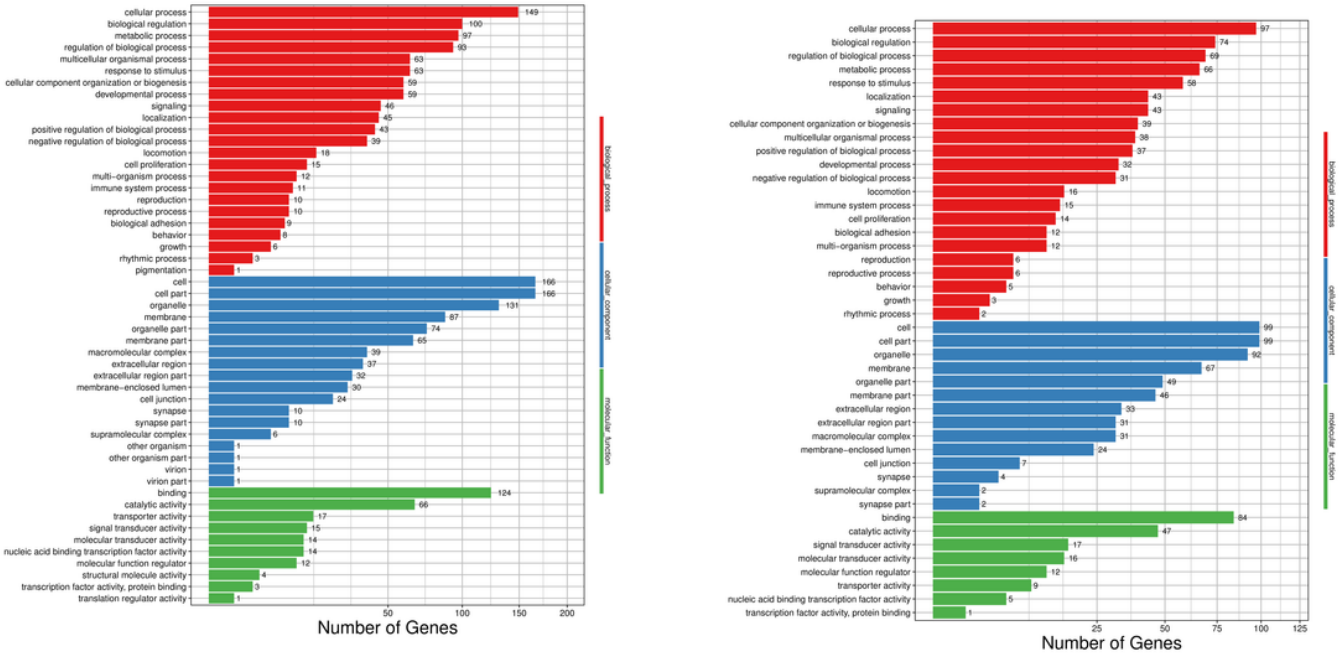

Figure 6

GO functional classification of DEGs for each pairwise comparison. (A) Follicular cyst vs. control groups. (B) Corpus luteum cyst vs. control groups. The x-axis indicates the number of DEGs (represented by its square root value). The y-axis represents GO terms. All GO terms are grouped into three ontologies; (blue = biological process, green = cellular component, red = molecular function).

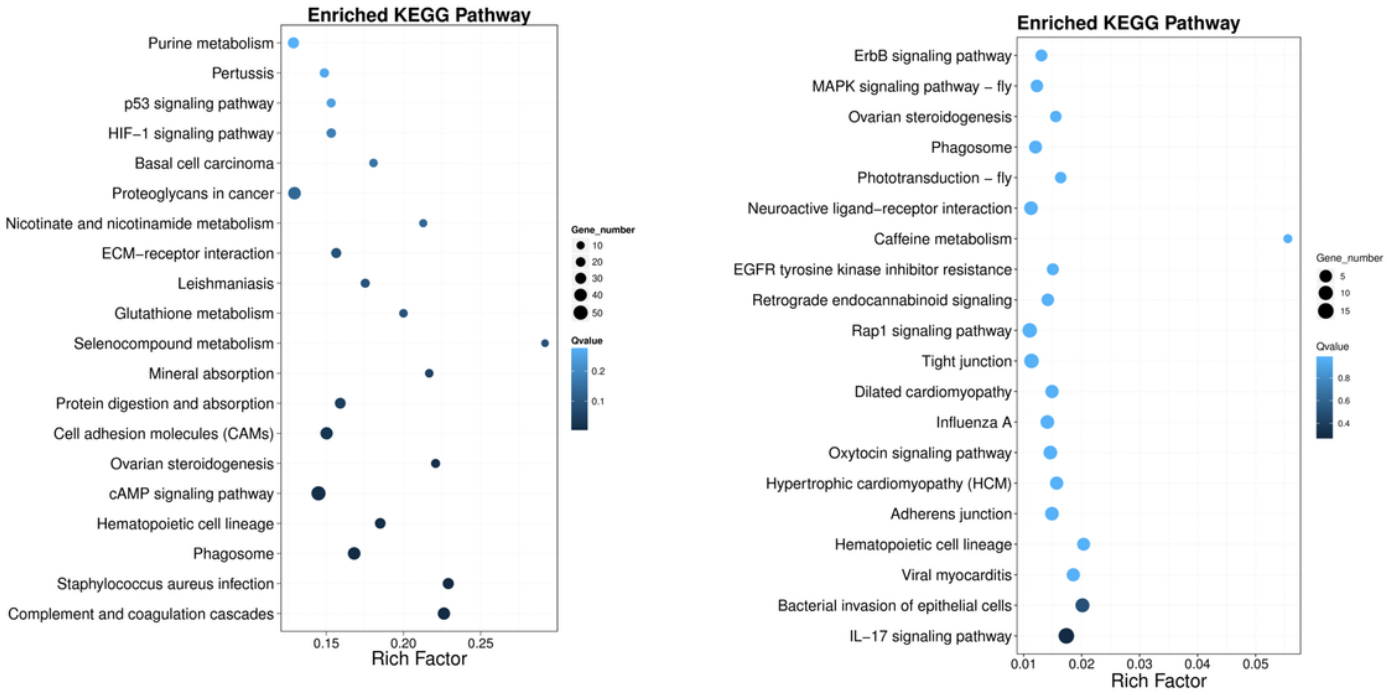

Figure 7

Pathway enrichment for DEGs identified in pairwise comparisons. (A) Follicular cyst vs. control groups. (B) Corpus luteum cyst vs. control groups. The Rich Factor is the ratio of the number of DEGs annotated in a given pathway term relative to the total number of genes annotated in the pathway term. A larger Rich Factor indicates greater intensity. The Q-value is the corrected p-value ranging from 0 to 1. A lower Q-value indicates greater intensity. The top 20 enriched pathway terms are displayed.